Available online at www.sciencedirect.com
ScienceDirect
Trans. Nonferrous Met. Soc. China 25(2015) 2253−2259
Transactions of Nonferrous Metals Society of China
www.tnmsc.cn

Synthesis of $Ni_{0.8}Co_{0.1}Mn_{0.1}(OH)_2$ precursor and electrochemical performance of $LiNi_{0.8}Co_{0.1}Mn_{0.1}O_2$ cathode material for lithium batteries

Yue HUANG, Zhi-xing WANG, Xin-hai LI, Hua-jun GUO, Jie-xi WANG

School of Metallurgy and Environment, Central South University, Changsha 410083, China

Received 2 September 2014; accepted 3 March 2015

Abstract: Spherical and homogeneously mixed metal hydroxide $Ni_{0.8}Co_{0.1}Mn_{0.1}(OH)_2$ precursor was successfully synthesized by co-precipitation method in a simple and small vessel with the volume of 1 L. The conditions of synthetic process including amount of chelating agent, stirring speed and temperature were studied. $LiNi_{0.8}Co_{0.1}Mn_{0.1}O_2$ samples were obtained by calcinating the precursors. The crystal structure, morphology and electrochemical properties were investigated by X-ray diffraction (XRD), scanning electron microscopy (SEM), charge−discharge test, AC impedance and cyclic voltammetry. In the voltage range of 2.8−4.3 V, the initial discharge capacities of $LiNi_{0.8}Co_{0.1}Mn_{0.1}O_2$ at 0.1*C* and 1*C* rates were 199 and 170 mA·h/g, respectively. After 80 cycles at 1*C*, the discharge capacity retention was 92%, suggesting its promising application as the cathode material for Li-ion batteries.
Key words: lithium-ion batteries; cathode material; co-precipitation; electrochemical properties

1 Introduction

Layered $LiNi_{1-x-y}Co_xMn_yO_2$(LNCM) exhibits high capacity, good cycling stability and low cost, and has been considered to be a promising cathode material for automobile applications such as plug-in hybrid vehicles (PHEVs) and electric vehicles (EVs) [1–3]. Among these layered materials, $LiNi_{0.8}Co_{0.1}Mn_{0.1}O_2$ shows a relatively high capacity than $LiNi_{1/3}Co_{1/3}Mn_{1/3}O_2$ and $LiNi_{0.6}Co_{0.2}Mn_{0.2}O_2$ due to the high content of Ni which is the main active redox species ($Ni^{2+}\leftrightarrow Ni^{4+}$) in the host structure [4−6].

Great efforts have been made toward the synthesis of Ni-rich materials [7,8]. Previous work proved that it is difficult to prepare high amount of Ni contented compounds, partly due to the sensitivity to synthesis condition. The synthesis process needs to be operated under stable environment with precise control, and there have been some reports that high Ni-content spherical material can be successfully synthesized by using adjusted reactors with large capacity [9,10]. However, there is no report that high Ni-content spherical composite materials with good performance can be synthesized by using simple and small reactors.

In this work, high Ni-content precursors were synthesized in a relatively simple and small reactor with capacity of about 1 L. The synthesis conditions including stirring speed, temperature and amount of chelating agent have been investigated. After co- precipitation, spherical and homogeneously mixed metal hydroxide $Ni_{0.8}Co_{0.1}Mn_{0.1}(OH)_2$ were successfully synthesized. Then $LiNi_{0.8}Co_{0.1}Mn_{0.1}O_2$ with good electrochemical performance was synthesized from the precursor by calcination under oxygen atmosphere.

2 Experimental

2.1 Sample preparations

The progress of preparing $Ni_{0.8}Co_{0.1}Mn_{0.1}(OH)_2$ is graphically presented in Fig. 1. $NiSO_4·6H_2O$, $CoSO_4·7H_2O$ and $MnSO_4·H_2O$ were used as starting materials and were dissolved in distilled water in a mole ratio of $n(Ni^{2+}):n(Co^{2+}):n(Mn^{2+})$=8:1:1, and the total metal ions concentration is 1 mol/L. Subsequently, this solution was slowly pumped into a reactor (1 L) with continuous stirring under nitrogen atmosphere. Simultaneously, a 2 mol/L NaOH solution and an appropriate amount of NH_4OH solution as chelating agent were also pumped into the reactor together. After that, the precipitate was filtered and washed several times

Foundation item: Project (2014CB643406) supported by the National Basic Research Program of China
Corresponding author: Zhi-xing WANG; Tel/Fax: +86-731-88836633; E-mail: zxwang@csu.edu.cn
DOI: 10.1016/S1003-6326(15)63838-9

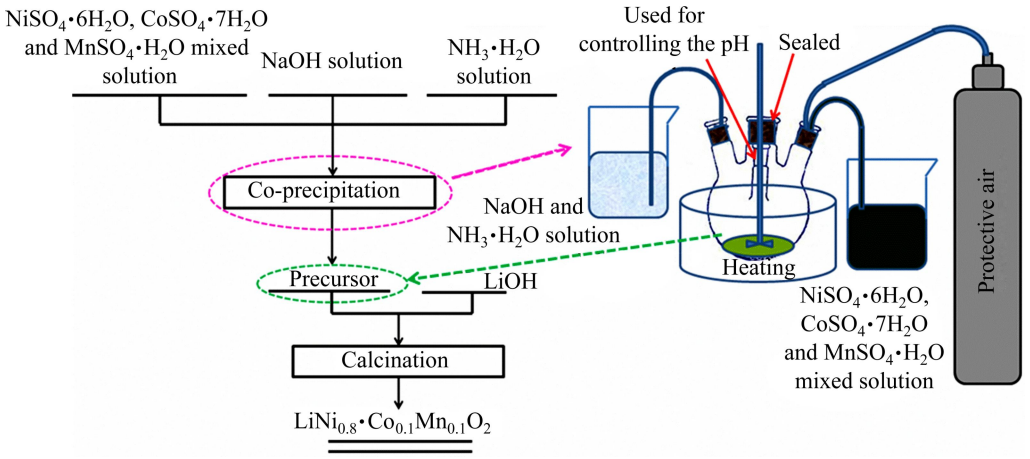

Fig. 1 Experimental procedure and apparatus

with distilled water to remove the residual ions (Na^+, SO_4^{2-} and other ions). The precipitate was then dried at 80 °C overnight. The concentration of the solution, pH (the pH value was controlled at 11.25), the amount of NH_4OH, stirring speed and temperature in the reactor were carefully controlled. The obtained $Ni_{0.8}Co_{0.1}Mn_{0.1}(OH)_2$ precursor was mixed with $LiOH·H_2O$ in a mole ratio of 1:1.05 and thoroughly ground. Then, the mixture was sintered at 480 °C for 5 h followed by at 750 °C for 15 h in flowing oxygen atmosphere.

2.2 Sample characterization

X-ray diffraction (XRD) was carried out with a diffractometer D/max 2550 X (Rigaku, Japan), using Cu K_α radiation (λ=0.154056 nm, voltage 40 kV, and current 300 mA), with a step size of 0.02° and a recorded range from 10° to 80°. The SEM images and elemental mapping of the particles were observed with scanning electron microscope (SEM, JEOL, JSM-5600LV).

2.3 Electrochemical performance evaluation

The electrodes for electrochemical studies were fabricated from a mixture of the active material, super P and poly(vinylindene fluoride) at a mass ratio of 8:1:1. The mixture was dispersed in N-methyl pyrrolidinone (NMP) and stirred to form viscous slurry, which was then coated onto Al foil using a doctor-blade. After drying at 120 °C for 12 h, the film was punched into disks with a diameter of 12 mm. Then, the disks were vacuum dried at 60 °C for 12 h, cooled and transferred into an argon-filled glove-box, followed by being assembled into CR2025 coin-type cells with a negative electrode of Li foil and electrolyte (1 mol/L $LiPF_6$ in *m*(EC):*m*(EMC):*m*(DMC)=1:1:1). The charge–discharge tests were implemented between 2.8 and 4.3 V at a desired rate (1*C* corresponds to 200 mA/g). Before cycling tests, all the cells were sequentially activated at 0.1*C* , 0.2*C* and 0.5*C* for two cycles, respectively, and then cycled at 1*C* rate in the following 100 cycles at 25 °C. Cyclic voltammogram (CV) measurements were done by a CHI660A electrochemical workstation between 2.8 and 4.3 V at a scan rate of 0.1 mV/s. AC impedance was tested on the same electrochemical workstation over the frequency range of 0.01 Hz to 100 kHz.

3 Results and discussion

3.1 Optimization of synthetic conditions of $Ni_{0.8}Co_{0.1}Mn_{0.1}(OH)_2$

The spherical $Ni_{0.8}Co_{0.1}Mn_{0.1}(OH)_2$ precursor with a very homogeneous distribution of Ni^{2+}, Co^{2+} and Mn^{2+} on the atomic scale can be synthesized via the co-precipitation method [9,11−14]. And it is easier to synthesize $LiNi_{0.8}Co_{0.1}Mn_{0.1}O_2$ from $Ni_{0.8}Co_{0.1}Mn_{0.1}(OH)_2$ precursor because they share very similar layered structure which has been indicated by the X-ray diffraction patterns [6,12]. During the synthetic process, the pH, stirring speed, temperature and amount of chelating agent are crucial factors [11–14]. In this research, series of experiments were operated by changing three critical factors including different concentrations of NH_4OH, stirring speeds and temperatures. And five representative experiments were picked out and listed in Table 1 to illustrate the effects of synthesis conditions on the physical and electrochemical

Table 1 Preparation conditions of $Ni_{0.8}Co_{0.1}Mn_{0.1}(OH)_2$ powders

Sample	Concentration of NH_4OH/(mol·L^{-1})	Temperature/ °C	Stirring speed/(r·min^{-1})
S_1	1	55	600
S_2	1	55	700
S_3	2	55	600
S_4	2	50	600
S_5	2	58	800

properties of the cathodes. $Ni_{0.8}Co_{0.1}Mn_{0.1}(OH)_2$ samples which were prepared under different conditions were labeled as S_i(i=1, 2, 3, 4, 5).

The pH value might change the composition of materials by affecting the formation of manganese compounds [15,16]. For example, excess of alkali during precipitation reaction facilitates the formation of some kinds of manganese oxides, so the pH value plays an important role to decide the purity of metal hydroxide [9]. Based on the former experiments (which are not shown here), the value of pH is 11.25 [12].

Figure 2 shows the SEM images of the $Ni_{0.8}Co_{0.1}Mn_{0.1}(OH)_2$ powders of S_1, S_2, S_3, S_4 and S_5, prepared at different conditions listed in Table 1.

Speeding up stirring rate can intensify the collision not only between the particles themselves but also between the particles and the vessel wall. That is beneficial to forming uniform and homogeneous spherical particles. Compared with sample S_1, sample S_2 was prepared at higher stirring speed (700 r/min), which suppressed the irregular agglomeration of the particles.

It is well known that NH_3 molecules play an important role on promoting the formation of $Ni_{0.8}Co_{0.1}Mn_{0.1}(OH)_2$ powders. Single phases of $Ni(OH)_2$, $Co(OH)_2$ or $Mn(OH)_2$ would form and exist as impurity phase in the final product if the chelating agent of NH_4OH was not employed [17]. Samples S_1 and S_3 were prepared with different concentrations of NH_4OH as described in Table 1. With a low concentration of NH_4OH (see S_1), irregular particles result in serious agglomeration due to the existence of a lot of vacancies among particles and the bad fluidity of the powders. With a higher concentration of NH_4OH (sample S_3), the particles become homogenous, small and quasi-spherical.

High temperature is beneficial for the formation of Mn contained hydroxide, however, when the temperature is higher than 60 °C, $Mn(OH)_2$ tends to be oxidized to MnO(OH) [9]. The SEM images of the samples S_3 and S_4 show that comparatively higher temperature facilitates the growth of secondary particles. As shown in Fig. 2,

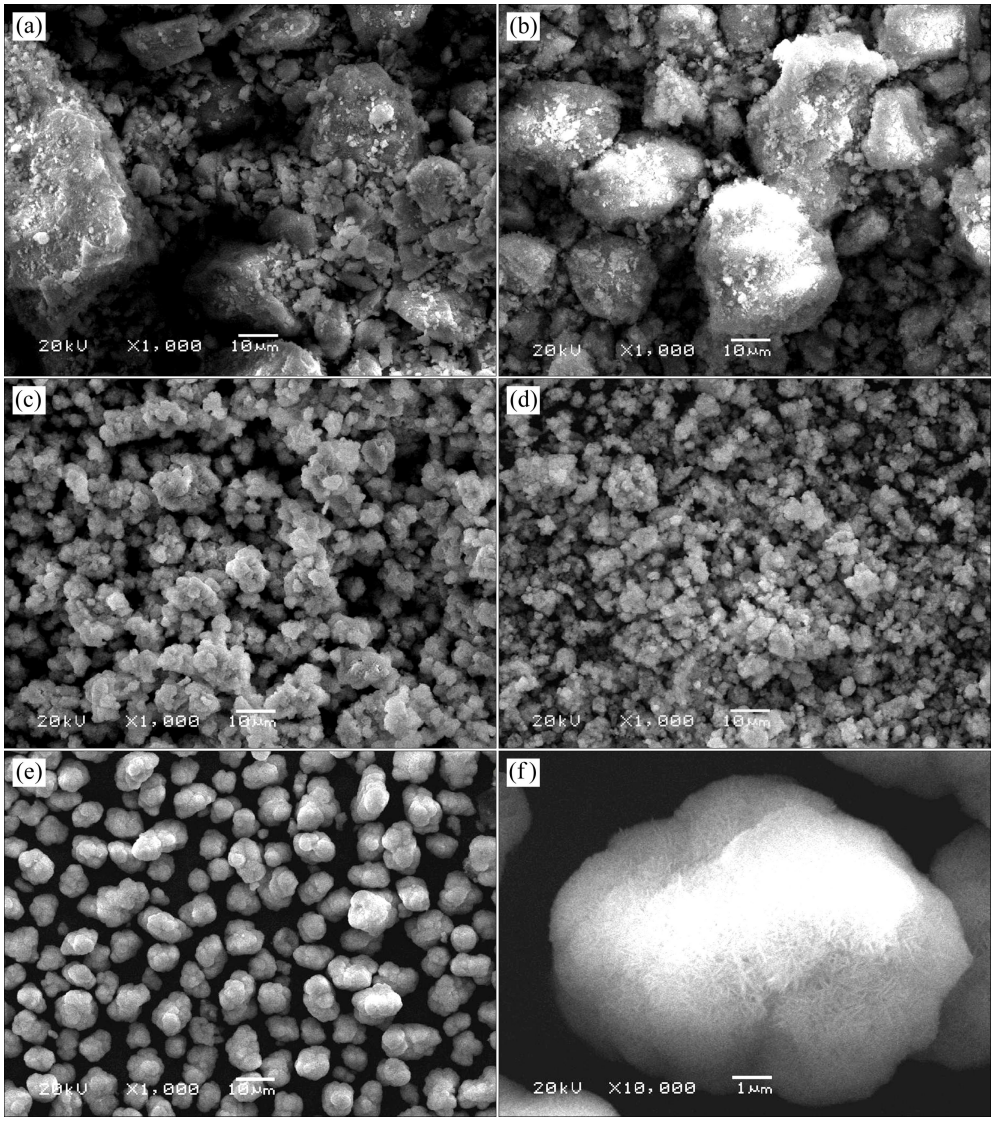

Fig. 2 SEM images of $Ni_{0.8}Co_{0.1}Mn_{0.1}(OH)_2$ powders prepared at different conditions: (a) S_1; (b) S_2; (c) S_3; (d) S_4; (e, f) S_5

sample S_5 prepared with higher temperature (58 °C), higher stirring speed (800 r/min) and high concentration of NH_4OH (2 mol/L) exhibits more uniform morphology. Under this condition, the particles are nearly spherical in shape. This result is consistent with the previous studies, that relatively high temperature and stirring speed with appropriate amount of NH_4OH and value of pH facilitate the formation of uniform and spherical particles [9,10,12].

3.2 Preparation of $LiNi_{0.8}Co_{0.1}Mn_{0.1}O_2$

Figure 3 displays the XRD patterns of the five $LiNi_{0.8}Co_{0.1}Mn_{0.1}O_2$ samples synthesized from the precursors S_i (i=1, 2, 3, 4, 5). $LiNi_{0.8}Co_{0.1}Mn_{0.1}O_2$ samples were labelled as S'_i (i=1, 2, 3, 4, 5) in order to distinguish from the corresponding precursors. The results reveal that all peaks are indexed as hexagonal a-$NaFeO_2$ structure with a space group of $R\bar{3}m$ and no extra diffraction peaks exist. As can be seen, all the XRD patterns show clear splits between the 006/012 and 108/110 peaks, which means that the materials have obvious hexagonal structure [6,18].

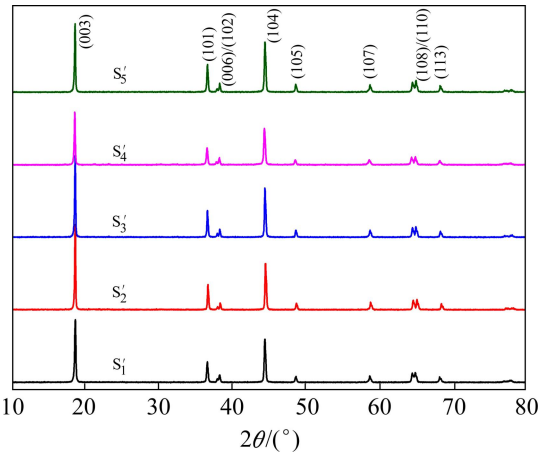

Fig. 3 XRD patterns for $LiNi_{0.8}Co_{0.1}Mn_{0.1}O_2$ samples prepared at 750 °C

3.3 Electrochemical properties of $LiNi_{0.8}Co_{0.1}Mn_{0.1}O_2$ materials

Figure 4(a) exhibits the initial charge–discharge curves of the synthesized $LiNi_{0.8}Co_{0.1}Mn_{0.1}O_2$ samples at a current density of 0.1C at room temperature. All the cells show very smooth curves. However, different samples deliver different discharge capacities. The initial discharge capacities for sample S'_1 to S'_5 are 174, 164, 180, 187, and 199 mA·h/g, respectively. And the corresponding coulombic efficiencies are 78%, 81%, 82%, 87% and 86%, respectively.

Figure 4(b) presents the cycle performance of the obtained $LiNi_{0.8}Co_{0.1}Mn_{0.1}O_2$ samples at 1C at room temperature. The discharge capacities of all the samples

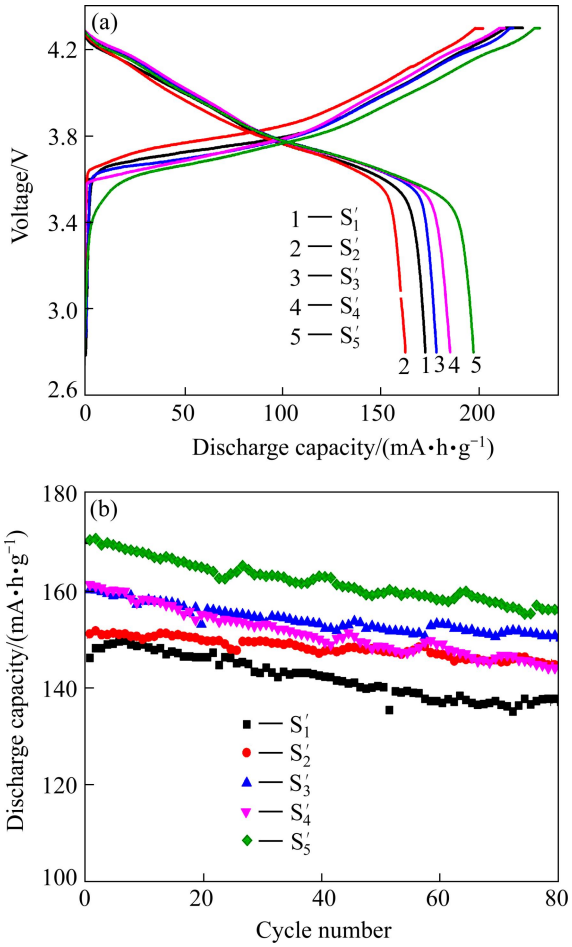

Fig. 4 Initial charge–discharge curves (a) and discharge capacities as function of number of cycle (b) in voltage range of 2.8–4.3 V at 1C rate at 25 °C of $LiNi_{0.8}Co_{0.1}Mn_{0.1}O_2$

tend to decrease slowly with the increase of the cycle number. The capacity retentions for samples S'_1 to S'_5 are 94%, 95%, 93%, 89% and 92% after 80 cycles, respectively. Sample S'_2 exhibits the highest capacity retention but low initial capacity. Considering both capacity and capacity retention rate, sample S'_5 owns better electrochemical performance than the others.

Here, sample S'_5 was picked up to examine the composition and the uniformity on the surface of the particles by using energy dispersive X-ray spectroscopy (EDX). It is seen from Fig. 5 that the Ni, Co and Mn elements are uniformly distributed on the particles' surface. Moreover, it can be found that the spherical shape and the size of secondary particle are maintained after calcination (Fig. 5(b)). The mole ratio of n(Ni):n(Co): n(Mn) is nearly 8:1:1, which is consistent with the initial designed composition. The result also proves that homogeneously mixed metal hydroxide $Ni_{0.8}Co_{0.1}Mn_{0.1}(OH)_2$ is synthesized.

Figure 6 shows the rate capacity of sample S'_5 between the voltage of 2.8−4.3 V. The cell was cycled at

0.1*C* 0.2*C*, 0.5*C*, 1*C*, 2*C* and 5*C* rates sequentially with 10 cycles for each current density. The cell delivers discharge capacities of 196, 185, 175, 163, 152 and 127 mA·h/g at 0.1*C*, 0.2*C*, 0.5*C*, 1*C*, 2*C* and 5*C* rates, respectively. As seen in Fig. 6(b), after being cycled at 5*C*, the capacity shows no capacity fading when the current density was back to 0.1*C*.

Electrochemical impedance spectroscopy (EIS) was measured after different cycles at charge state (Fig. 7(a)). The Nyquist plots are fitted using the equivalent circuit model (inset Fig. 7(a)) and the fitting parameters are listed in Table 2. R_{sf} stands for surface film impedance and R_{ct} stands for electrolyte/oxide reaction resistance. This model includes the Ohmic resistance (R_e) of the cell, the surface film impedance (R_{sf}//CPE_{sf}), electrolyte/oxide reaction resistance (R_{ct}//CPE_{dl}), and the Warburg impedance (Z_w). Table 2 shows that the surface film resistance is nearly stable and electrolyte/oxide reaction resistance gradually increases upon further cycling. The stability of R_{sf} is due to the stable solid−electrolyte interface (SEI) film which was formed on the surface of the electrode after activation. The subsequent continuous increasing in R_{ct} confirms that the impedance increases slowly with the increasing of cycles.

Cyclic voltammetries of the sample S'_5 between 2.8 and 4.3 V at a scan rate of 0.1 mV/s for the first, second and third cycle were carried out to investigate the structural stability of $LiNi_{0.8}Co_{0.1}Mn_{0.1}O_2$, as shown in Fig. 7(b). It can be seen that three redox couples exist in the cyclic voltammogram curves, a sharp oxidation peak and two secondary peaks, illustrating that phase transitions exist from hexagonal to monoclinic in the

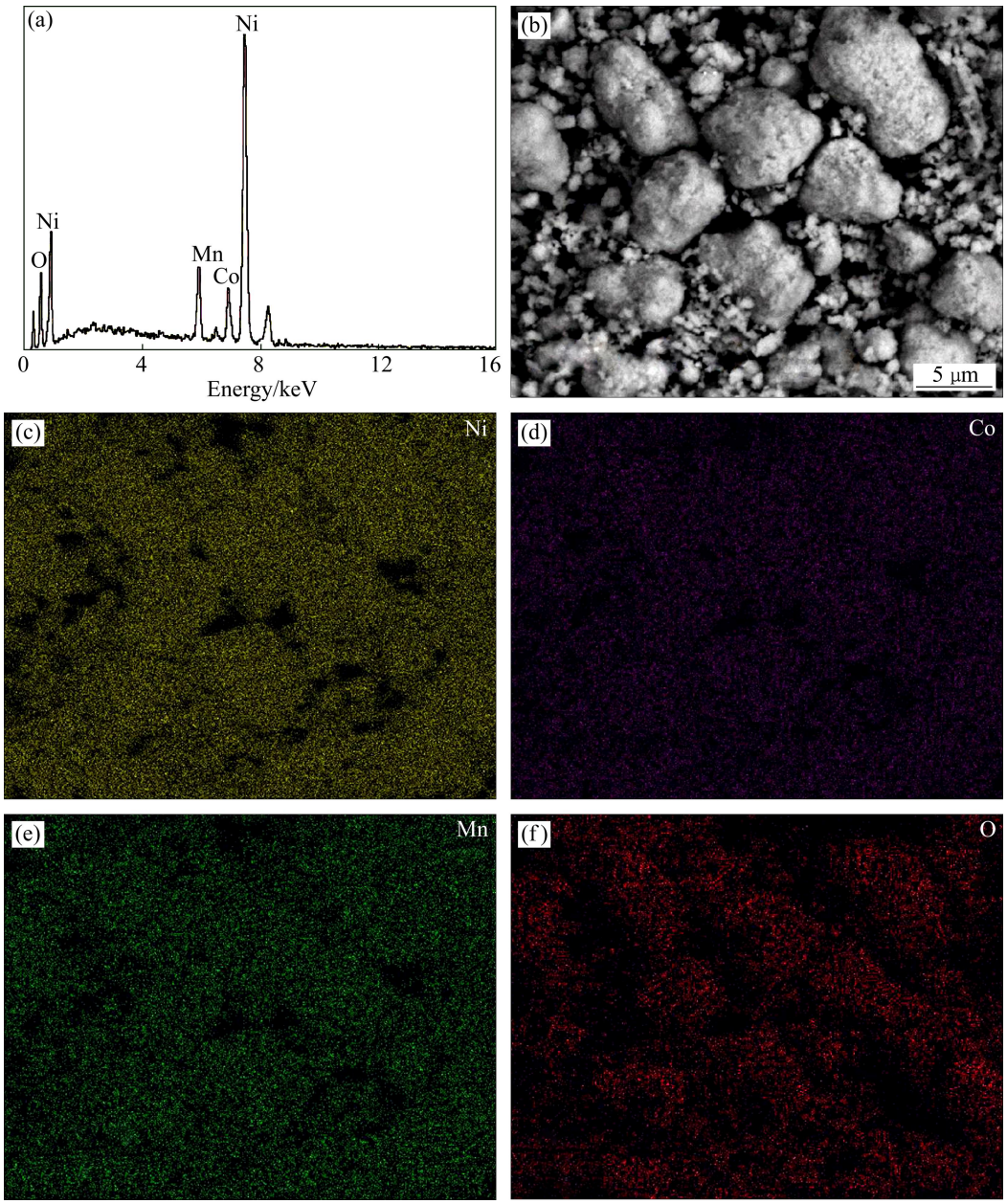

Fig. 5 EDX spectrum (a), SEM image (b) and elemental mappings (c−f) of sample S'_5

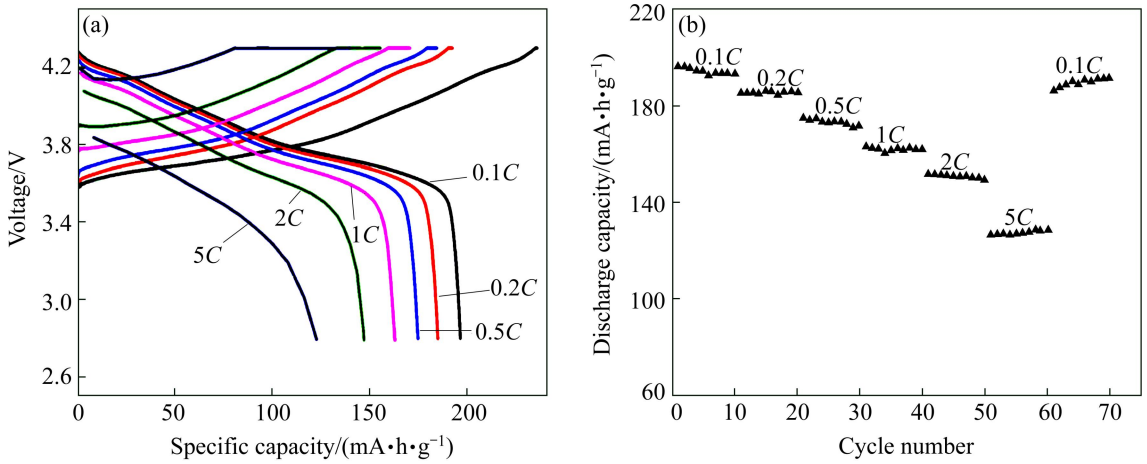

Fig. 6 Charge−discharge curves at different rates (a) and rate capacity curves (b) of sample S_5

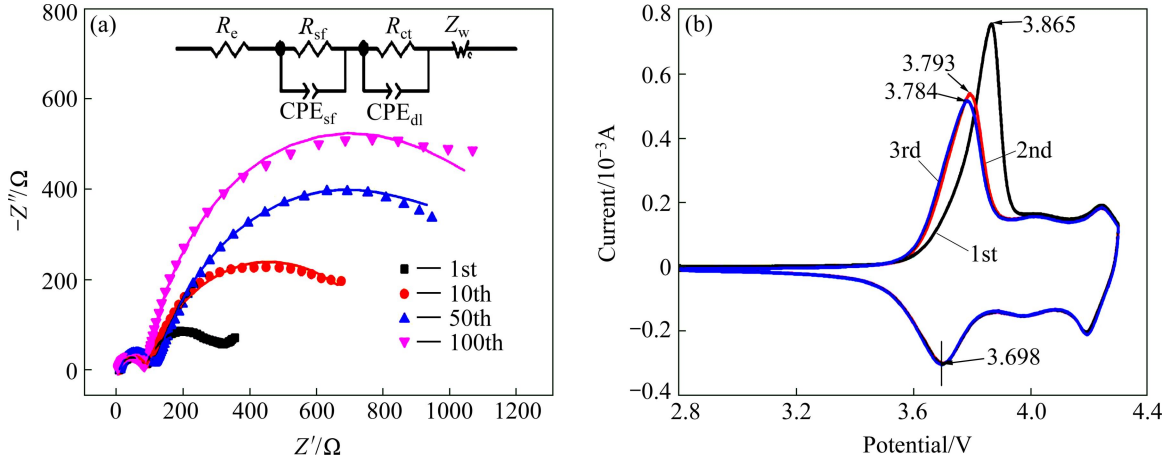

Fig. 7 Nyquist plots after different cycles (a) and cyclic voltammogram curves (b) of sample S_5'

Table 2 Impedance parameters for sample S_5' recorded after different cycle numbers

Cycle number	R_{sf}/Ω	R_{ct}/Ω
1	82	200
10	80	683
50	100	855
100	75	918

voltage range of 2.8–4.3 V [19,20]. It is clearly shown in Fig. 7(b) that the major anodic peak shifts from 3.865 V at the first cycle to 3.793 V and 3.784 V at the second and third cycle, respectively, while their corresponding redox reaction gaps are 0.167, 0.095 and 0.086 V. However, there is no obvious difference in the cathodic peaks (3.698 V). This phenomenon may be partially attributed to the cation mixing in the first cycle [12]. After the first cycle, the curves of the second and third cycle almost overlap. This demonstrates the good reversibility of Li^+ ions during intercalating and de-intercalating in compound and the high electrochemical performance.

4 Conclusions

1) Spherical and homogeneous $Ni_{0.8}Co_{0.1}Mn_{0.1}(OH)_2$ were successfully synthesized in round bottom flask with four necks (1 L) by co- precipitation method.

2) The as-prepared $LiNi_{0.8}Co_{0.1}Mn_{0.1}O_2$ electrode shows a good cycling stability which exhibits discharge capacity of 199 mA·h/g at a current density of 20 mA/g, and initial discharge capacity of 170 mA·h/g at 1C rate with capacity retention of 92% after 80 cycles, as well as excellent rate capability.

3) These results indicate that high-performance $LiNi_{0.8}Co_{0.1}Mn_{0.1}O_2$ cathode materials can be synthesized in small reactor by co-precipitation method, and this is a simple but efficient synthesis route for high Ni material.

References

[1] SHIM J, KOSTECKI R, RICHARDSON T, SONG X, STRIEBEL K. Electrochemical analysis for cycle performance and capacity fading of a lithium-ion battery cycled at elevated temperature [J]. Journal of Power Sources, 2002, 112(1): 222−230.

[2] BELHAROUAK I, SUN Y K, LIU J, AMINE K. $Li(Ni_{1/3}Co_{1/3}Mn_{1/3})O_2$ as a suitable cathode for high power applications [J]. Journal of Power Sources, 2003, 123(2): 247−252.

[3] YABUUCHI N, OHZUKU T. Novel lithium insertion material of $LiCo_{1/3}Ni_{1/3}Mn_{1/3}O_2$ for advanced lithium-ion batteries [J]. Journal of Power Sources, 2003, 119: 171−174.

[4] CHO J, KIM T J, KIM J, NOH M, PARK B. Synthesis, thermal, and electrochemical properties of $AlPO_4$-coated $LiNi_{0.8}Co_{0.1}Mn_{0.1}O_2$ cathode materials for a Li-ion cell [J]. Journal of The Electrochemical Society, 2004, 151(11): A1899−A1904.

[5] KIM M H, SHIN H S, SHIN D, SUN Y K. Synthesis and electrochemical properties of $Li[Ni_{0.8}Co_{0.1}Mn_{0.1}]O_2$ and $Li[Ni_{0.8}Co_{0.2}]O_2$ via co-precipitation [J]. Journal of Power Sources, 2006, 159(2): 1328−1333.

[6] NOH H J, YOUN S, YOON C S, SUN Y K. Comparison of the structural and electrochemical properties of layered $Li[Ni_xCo_yMn_z]O_2$ (x=1/3, 0.5, 0.6, 0.7, 0.8 and 0.85) cathode material for lithium-ion batteries [J]. Journal of Power Sources, 2013, 233: 121−130.

[7] SUN Bin, SHEN Guo-pei, HU Yan-long. High-rate capability of spinel $LiNi_{0.05}Mn_{1.95}O_4$ cathode for Li-ion batteries prepared via coprecipitated precursor [J]. Transactions of Nonferrous Metals Society of China, 2007, 17(S1): s937−s940.

[8] LI Ling-jun, LI Xin-hai, WANG Zhi-xing, WU Ling, ZHENG Jun-chao, LI Jin-hui. Synthesis of $LiNi_{0.8}Co_{0.1}Mn_{0.1}O_2$ cathode material by chloride co-precipitation method [J]. Transactions of Nonferrous Metals Society of China, 2010, 20(S1): s279−s282.

[9] LEE M H, KANG Y J, MYUNG S T, SUN Y K. Synthetic optimization of $Li[Ni_{1/3}Co_{1/3}Mn_{1/3}]O_2$ via co-precipitation [J]. Electrochimica Acta, 2004, 50(4): 939−948.

[10] LIANG Long-wei, DU Ke, PENG Zhong-dong, CAO Yan-bing, DUAN Jian-guo, JIANG Jian-bing, HU Guo-rong. Co-precipitation synthesis of $Ni_{0.6}CO_{0.2}Mn_{0.2}(OH)_2$ precursor and characterization of $LiNi_{0.6}CO_{0.2}Mn_{0.2}O_2$ cathode material for secondary lithium batteries [J]. Electrochimica Acta, 2014, 130: 82−89.

[11] LIU Zhao-lin, YU Ai-shui, LEE J Y. Synthesis and characterization of $LiNi_{1-x-y}Co_xMn_yO_2$ as the cathode materials of secondary lithium batteries [J]. Journal of Power Sources, 1999, 81: 416−419.

[12] LI Ling-jun, LI Xin-hai, WANG Zhi-xing, GUO Hua-jun, YUE Peng, CHEN Wei, WU Ling. A simple and effective method to synthesize layered $LiNi_{0.8}Co_{0.1}Mn_{0.1}O_2$ cathode materials for lithium ion battery [J]. Powder Technology, 2011, 206(3): 353−357.

[13] PAN Cheng-chi, BANKS C E, SONG Wei-xin, WANG Chi-wei, CHEN Qi-yuan, JI Xiao-bo. Recent development of $LiNi_xCo_yMn_zO_2$: Impact of micro/nano structures for imparting improvements in lithium batteries [J]. Transactions of Nonferrous Metals Society of China, 2013, 23(1): 108−119.

[14] HU Chuan-yue, GUO Jun, DU Yong, XU Hong-hui, HE Yue-hui. Effects of synthesis conditions on layered $Li[Ni_{1/3}Co_{1/3}Mn_{1/3}]O_2$ positive-electrode via hydroxide co-precipitation method for lithium-ion batteries [J]. Transactions of Nonferrous Metals Society of China, 2011, 21(1): 114−120.

[15] YU Xiao-yuan, HU Guo-rong, PENG Zhong-dong, XIAO Jin, LIU Ye-xiang. Synthesis and electrochemical characterization of layered $Li[Ni_{1/3}Co_{1/3}Mn_{1/3}]O_2$ cathode material for Li-ion batteries [J]. Transactions of Nonferrous Metals Society of China, 2005, 15(6): 1425−1428.

[16] ZHANG Chuan-fu, YANG Ping, DAI Xi, XIONG Xuan, ZHAN Jing, ZHANG Yin-liang. Synthesis of $LiNi_{1/3}Co_{1/3}Mn_{1/3}O_2$ cathode material via oxalate precursor [J]. Transactions of Nonferrous Metals Society of China, 2009, 19(3): 635−641.

[17] LI De-cheng, SASAKI Y, KAGEYAMA M, KOBAYAKAWA K, SATO Y. Structure, morphology and electrochemical properties of $LiNi_{0.5}Mn_{0.5-x}Co_xO_2$ prepared by solid state reaction [J]. Journal of Power Sources, 2005, 148: 85−89.

[18] LI Yan, LIU Kai-yu, LÜ Mei-yu, WEI Lai, ZHONG Jian-jian. Synthesis, characterization and electrochemical performance of AlF_3-coated $Li_{1.2}(Mn_{0.54}Ni_{0.16}Co_{0.08})O_2$ as cathode for Li-ion battery [J]. Transactions of Nonferrous Metals Society of China, 2014, 24(12): 3534−3540.

[19] LI W, REIMERS J N, DAHN J R. In situ X-ray diffraction and electrochemical studies of $Li_{1-x}NiO_2$ [J]. Solid State Ionics, 1993, 67(1): 123−130.

[20] WOO S U, YOON C S, AMINE K, BELHAROUAK I, SUN Y K. Significant improvement of electrochemical performance of AlF_3-coated $Li[Ni_{0.8}Co_{0.1}Mn_{0.1}]O_2$ cathode materials [J]. Journal of The Electrochemical Society 2007, 154(11): A1005−A1009.

锂离子电池正极材料 $LiNi_{0.8}Co_{0.1}Mn_{0.1}O_2$ 及其前驱体的制备和性能

黄 越，王志兴，李新海，郭华军，王接喜

中南大学 冶金与环境学院，长沙 410083

摘 要：通过共沉淀法在体积为 1 L 的简易烧杯中合成具有球形形貌的层状前驱体 $Ni_{0.8}Co_{0.1}Mn_{0.1}(OH)_2$。探讨合成过程中影响因素，包括络合剂用量、搅拌速度和反应温度对产物形貌和性能的影响。通过高温烧结前驱体合成 $LiNi_{0.8}Co_{0.1}Mn_{0.1}O_2$ 材料。用扫描电子显微镜(SEM)和 X 射线衍射仪(XRD)对材料的形貌和晶体结构进行表征，通过充放电测试、交流阻抗和循环伏安法研究材料的电化学性能。在 2.8−4.3 V 电压范围内，合成的 $LiNi_{0.8}Co_{0.1}Mn_{0.1}O_2$ 在 0.1C 和 1C 倍率下的首次放电容量分别为 199 和 170 mA·h/g。在 1C 下循环 80 次后，其容量保持率为 92%，表明这是一种具有良好应用前景的锂离子电池正极材料。

关键词：锂离子电池；正极材料；共沉淀法；电化学性能

(Edited by Yun-bin HE)